Pores Formed by Bis-macrocyclic Bola-amphiphiles in Vesicle and Planar Bilayer Membranes

T. M. Fyles,* D. Loock, W. F. van Straaten-Nijenhuis, and X. Zhou

Department of Chemistry, University of Victoria, Victoria, British Columbia V8W 3P6, Canada

Received July 5, 1996[⊗]

A new series of bis-macrocyclic bola-amphiphiles were prepared, and their transport activities in vesicle and planar bilayer membranes were evaluated. From vesicle experiments, the apparent kinetic order in transporter indicates that aggregates are the kinetically active species. Step-conductance changes observed in planar bilayer membranes indicate that the compounds act as channels. Multiple copies of the same channel form in which the conductance is controlled by the macrocyclic portions of the structures. The pores are ion-selective in the sequence $Cs^+ > K^+ > Na^+ > Cl^-$, controlled by the polar head-groups of the structures. The data are consistent with a model involving the formation of active dimers.

Cation transport across lipid bilayer membranes by synthetic ion channels has been achieved in a variety of ingenious ways over the past 15 years.[1] These reports draw inspiration from natural ion channels[2] or natural channel-forming oligopeptides[3] and often achieve overall *functional* similarity with natural transporters. The extent of *structural* similarity is much lower, due to a tremendous disparity in size and complexity between synthetic and biological transporters. Although artificial transport systems may illuminate details of the biological ion translocation process, an immediate potential is in applications to separations, pharmaceuticals, drug-delivery systems, sensors, and other devices.[4]

The creation of useful devices based on transport across bilayer membranes sets a number of unresolved challenges. Foremost among these is the question of transporter size. The active structures of synthetic transporters, small in comparison to natural examples, are nonetheless large by the standards of synthetic chemistry.[5] They must span a 4 nm thick bilayer and simultaneously surround an ion of at least 0.3 nm diameter. This can be achieved in a unimolecular structure, or more simply achieved via an aggregation of smaller subunits. Large unimolecular structures require efficient covalent assembly, either from modular components,[6] via controlled polymerization,[7] or by the optimized chemistry of polypeptide synthesis.[8] The aggregation of smaller subunits sets a less severe synthetic problem, but poses additional characterization difficulties. But which is better? Are unimolecular structures required to control transport rate and selectivity? Or can small aggregating systems do the job just as well with less synthetic effort?

The simplicity of examples apparently involving aggregates is very appealing. Führhop reported a number of bola-amphiphiles capable of forming pores in thin monomolecular vesicle membranes, presumably via aggregate structures.[9] Aggregate pore-formation by bola-amphiphiles in bilayer vesicle membranes has been reported by Regen[10] and by us.[11] In all these cases the marked dependence of transport rate on transporter concentration was taken as evidence of aggregate formation. Direct evidence of single channels in planar bilayers from simple surfactants has been reported by Kobuke,[12] but the evidence for aggregates is indirect. Ghadiri has reported the most structurally sophisticated aggregate channel to date—a columnar aggregate of cyclic peptides that defines a 0.5 nm pore.[13] This system is active in both vesicles and planar bilayers, shows single-channel openings, and shows spectral changes consistent with the proposed tubular aggregate. On the other hand, none of these systems show marked ion selectivity, although modest selectivity among alkali metal cations has been noted.[11,13] Cation selectivity is more frequently associated with unimolecular transporters,[1,7] as the effective pore-size is restricted by the transporter structure. Conversely, membrane-disrupting agents that open large defects in bilayer membranes are generally indiscriminate and unselective.[14]

Whatever size may be required, the structural requirements for efficient ion transport are now reasonably clear.[15] The transporter should be compatible with the bilayer membrane environment, possessing amphiphilic

* To whom correspondence should be addressed. Tel.: (604) 721-7184. Fax: (604) 721-7147. E-mail: tmf@uvaix.uvic.ca.

[⊗] Abstract published in *Advance ACS Abstracts,* November 15, 1996.

(1) For example, see: (a) Tanaka, Y.; Kobuke, Y.; Sokabe, M. *Angew. Chem., Int. Ed. Engl.* **1995**, *34*, 693. (b) Fyles, T. M.; Heberle, D.; van Straaten-Nijenhuis, W. F.; Zhou, X. *Supramol. Chem.* **1995**, *11*, 1 and references therein.

(2) *Carriers, Channels, and Pumps: An Introduction to Membrane Transport*; Stein, W., Ed.; Academic Press: San Diego, 1990.

(3) (a) Wooley, A. G.; Wallace, B. A. *J. Membr. Biol.* **1992**, *129*, 109. (b) Sansom, M. S. P. *Prog. Biophys. Molec. Biol.* **1991**, *55*, 139.

(4) Cross, G. G.; Fyles, T. M.; Montoya-Pelaez. P. J.; van Straaten-Nijenhuis, W. F.; Zhou, X. *ACS Symp. Ser.* **1994**, *561*, 38.

(5) Cross, G. G.; Fyles, T. M.; James, T. D.; Zojaji, M. *Synlett* **1993**, 449.

(6) Fyles, T. M.; James, T. D.; Pryhitka, A.; Zojaji, M. *J. Org. Chem.* **1993**, *58*, 7456.

(7) Roks, M. F. M.; Nolte, R. J. *Macromolecules* **1992**, *25*, 5398.

(8) (a) Montal, M.; Montal, M. S.; Tomich, J. M. *Proc. Natl. Acad. Sci. U.S.A.* **1990**, *87*, 6929. (b) Grove, A.; Mutter, M.; Rivier, J. E.; Montal, M. *J. Am. Chem. Soc.* **1993**, *115*, 5919. (c) Akerfeldt, K. S.; Lear, J. D.; Wasserman, Z. R.; Chung, L. A.; DeGrado, W. F. *Acc. Chem. Res.* **1993**, *26*, 191.

(9) (a) Führhop, J.-H.; Liman, U. *J. Am. Chem. Soc.* **1984**, *106*, 4643. (b) Führhop, J.-H.; Liman, U.; David, H. H. *Angew. Chem., Int. Ed. Engl.* **1985**, *24*, 339. (c) Führhop, J.-H.; Liman, U.; Koesling, V. *J. Am. Chem. Soc.* **1988**, *110*, 6840.

(10) (a) Stadler, E.; Dedek, P.; Yamashita, K.; Regen, S. L. *J. Am. Chem. Soc.* **1994**, *116*, 6677. (b) Deng, G.; Merritt, M.; Yamshita, K.; Janout, V.; Sadownik, A.; Regen, S. L. *J. Am. Chem. Soc.* **1996**, *118*, 3307.

(11) Fyles, T. M.; Kaye, K.; Pryhitka, A.; Tweddell, J.; Zojaji, M. *Supramol. Chem.* **1994**, *3*, 197.

(12) (a) Kobuke, Y.; Ueda, K.; Sokabe, M. *J. Am. Chem. Soc.* **1992**, 114, 7618. (b) Kobuke, Y.; Ueda, K.; Sokabe, M. *Chem. Lett.* **1995**, 435.

(13) Ghadiri, M. R.; Granja, J. R.; Buehler, L. K. *Nature* **1994**, *369*, 301.

(14) (a) Jayasuriya, N.; Bosak, S.; Regen, S. L. *J. Am. Chem. Soc.* **1990**, *112*, 5844. (b) Nagawa, Y.; Regen, S. L. *J. Am. Chem. Soc.* **1991**, *113*, 7237. (c) Liu, Y.; Regen, S. L. *J. Am. Chem. Soc.* **1993**, *115*, 708.

S0022-3263(96)01267-4 CCC: $12.00 © 1996 American Chemical Society

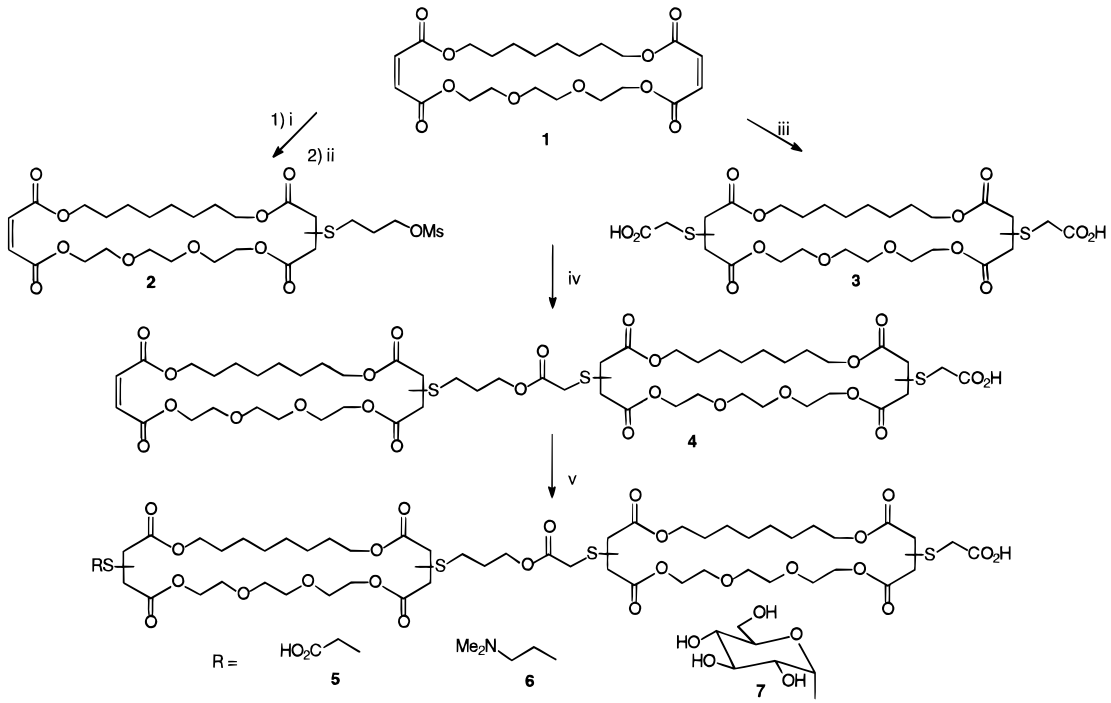

Figure 1. Synthesis of pore-formers. Conditions: (i) 3-mercaptopropanol, tetramethylpiperidine, 2-propanol, reflux, 2 h; (ii) MsCl, Et_3N, CH_2Cl_2, 0 °C, 2 h; (iii) 2-mercaptoacetic acid, tetramethylpiperidine, THF, 60 °C, 6 h; (iv) Me_4NOH, DMSO, 40 °C, 25 h; (v) thiol, tetramethylpiperidine, 40−60 °C, 6−16 h.

character and a roughly columnar shape to insert into the membrane in place of one or more lipid molecules. The transporter must also be capable of stabilizing an ion in transit across the nonpolar core of the bilayer membrane. This could involve direct ion-transporter interactions or might simply involve transporter stabilized water deep within the bilayer.

In order to achieve ion-selectivity using aggregate pore-formers, the size of the aggregate needs to be limited. We envisage dimers or trimers, closely similar to lipids in both cross-sectional area and chain length. Our previous bis-macrocyclic bola-amphiphiles were close to this goal, but the central linkage unit was quite bulky.[11] Fortunately, the modular synthetic chemistry underlying the system permits a reduction in the volume and functionality of the linker.[6,11] We report here on a combination of vesicle and planar bilayer techniques to explore the pore-forming properties of bola-amphiphiles similar to our previous work, but having a less bulky linkage. We will establish that this new series of compounds is substantially more active than the previous set and will probe the mechanism using a combination of techniques. This will provide a composite portrait of the channels formed by bis-macrocyclic bola-amphiphiles, which will partially respond to the questions posed above.

Results and Discussion

Synthesis of Transporters. The synthesis of candidate transporters is outlined in Figure 1. The procedures follow directly from previously reported work with this modular construction set.[6,11] The tetraester diene macrocycle **1** was converted to the mesylate **2** via the mono-Michael addition of 3-mercaptopropanol. Double-addition of 2-mercaptoacetic acid to **1** gave the diacid **3**, similar to longer homologs prepared by Fuhrhop[9] but which shows no tendency to form monomolecular membranes in aqueous solutions.

Mono-alkylation of **3** with **2** was achieved via the tetramethylammonium salt in DMSO. The ene acid **4** was accompanied by unreacted **3** and the expected higher molecular weight diene, the product of bis-alkylation. Purification was achieved using gel permeation chromatography on Sephadex LH-20 using 2-propanol/chloroform as eluent. This solvent composition afforded convenient separation but introduced an isopropyl ester as a chronic impurity. In this and subsequent steps, isopropyl esters account for minor peaks in the NMR (~2%). The corresponding molecular ions at +43 mass units in the −FAB-MS appear to be more abundant (up to 20% of the acid molecular ion intensity) due to favorable ionization of the esters. The ester impurity did not interfere with subsequent reactions.

The addition of a second head-group to form the bola-amphiphilic transporters **5**−**7** followed previously published procedures.[6,11] The products were purified by gel permeation chromatography, and the structures were established by NMR and FAB-MS. All compounds ran as a single component on an analytical gel permeation column under conditions where impurities differing by 50 g/mol could be resolved.

Transport Experiments: Vesicles. Vesicles were prepared by reverse evaporation from an 8:1:1 mixture of egg phosphatidyl choline:egg phosphatidic acid:cholesterol (PC:PA:Chol) in ether dispersed in a pH 6.6 buffer.[11,15] The vesicles were sized by filtration through Nucleopore membrane filters, and external buffer was replaced by unbuffered isomolal choline sulfate solution by gel filtration. Particle sizing by dynamic light scattering showed a bimodal distribution of vesicle sizes: 75−80% of the entrapped volume was associated with 350 nm diameter vesicles and the remainder with 130 nm diameter vesicles. Vesicle solutions were stable as

(15) Fyles, T. M.; James, T. D.; Kaye, K. C. *J. Am. Chem. Soc.* **1993**, *115*, 12315.

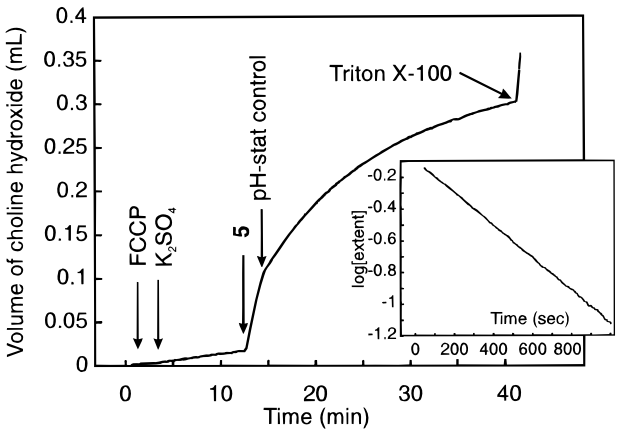

Figure 2. pH−stat curve of volume of choline hydroxide added as a function of time for compound **5** in vesicles. Details of the experiment are discussed in the text. Inset shows log (extent of transport) as a function of time after addition of **5**, showing first-order proton efflux from vesicles.

Table 1. Transport of Alkali Metal Cations by Pore-Formers[a]

trans-porter	[Tr] (mM)	rate × 10^9, mol H^+ s^{-1}					apparent kinetic order	normalized rate for K^+ [b] (×109, mol H^+ s^{-1})
		Li^+	Na^+	K^+	Rb^+	Cs^+		
7	14.5		2.4	2.2		1.9	1.9	4.8
6	21.6	2.8	2.9	2.5	3.0	3.0	2.1	2.5
5	20.7	0.9	1.0	2.1	1.5	1.1	1.7	2.4
4	21.2	1.0		1.3	1.3	1.2	2.0	1.5
8[c]	60[c]			0.9[c]			2.6[c]	0.06[c]

[a] Transport across vesicle membranes at 298 K in the presence of (8.1−8.4) × 10^{-7} M FCCP and (1.5−1.6) × 10^{-2} M M_2SO_4. [b] Normalized to [Tr] = 2.15 × 10^{-5} M, corresponding to 0.3 mol % Tr in lipid; normalized rate = (2.15 × 10^{-5}/[Tr])$^{\text{kinetic order}}$ × rate in the presence of K_2SO_4. [c] Reference 11; [K_2SO_4] = 0.049 M

prepared for periods of 2−3 days but were typically used within 36 h of preparation.

A transport experiment is illustrated in Figure 2. An aliquot of vesicle solution was suspended in unbuffered choline sulfate solution, and the pH was adjusted to 7.6 by addition of choline hydroxide solution under the control of a pH-stat titrimeter. This is the origin of the curve in Figure 2. A slow leakage of protons from the vesicles is evident, but the leakage is not accelerated by the addition of the proton carier FCCP or by the addition of potassium sulfate to the vesicle solution. Addition of transporter (**5** in this example) provokes an immediate release of protons from the vesicles. As shown previously,[11] this release is too rapid for the pH-stat titrimeter to follow, and a couple of minutes are required until the pH-stat control is established. Thereafter, there is a progressive proton efflux that eventually reaches a plateau. Controls established that proton release is not simply due to lysis by methanol. A typical experiment involves <1% methanol (vol/vol); no lysis is observed up to 2% methanol (vol/vol). At a late point in the experiment, the detergent Triton X-100 is added to release any remaining entrapped buffer. The inset to Figure 2 shows that the proton efflux follows a first-order process over the period where the titrimeter is controlling the pH gradient.

The activities of the compounds synthesised are summarised in Table 1 for different alkali metal cations. Previously published data for compound **8** (Chart 1) is included for comparison.[11] Rates have been normalized to 2.1 × 10^{-5} M, corresponding to 0.3 mol % transporter in lipid. It is conceivable that the more highly hydroxylated **8** is less active due to unfavorable partitioning to the vesicles. Previous work with **8** and its relatives showed that partition effects were relatively minor,[11] since compounds differing by up to 10 hydroxyl groups fell within 1 order of magnitude of equal activity. The 25−80-fold enhancement in rate for **4**−**7** relative to **8** is outside the range expected for a partition difference.

In terms of the active concentration range, compounds **4**−**7** are substantially more active than **8**. The apparent kinetic order in transporter in the presence of K^+ was determined from the dependence of log (initial rate) on log (transporter concentration)[10,11,15] for four concentrations between 5 and 30 μM. The values reported in Table 1 are about 2, indicating that an aggregate of transporters is the kinetically significant species in all cases. The apparent kinetic orders permit a normalization of the activities for the K^+ data. The rank order of activity shows **7** to be more active than either **5** or **6**, which are somewhat more active than **4**. This comparison shows **8** to be at least 25-fold less active than **4**, showing that the central linkage plays a significant role in determining overall activity.

The normalized activities are consistent with the previous rank ordering for the different head groups involved, but the small range of the effect shows that the head groups play a relatively minor role in determining activity. In fact, compound **4** is not a bola-amphiphile at all yet can induce efficient cation transport. The headgroups are more significant in determining cation selectivity, but the effects remain modest. Compound **5**, a dianion at the pH of the experiment, shows an Eisenman IV selectivity sequence, consistent with neutral oxygen donors interacting with the cations. It is important to reiterate[11,15] that the pH-stat experiment does not directly probe the ion translocation process. It simply probes the cation dependence of the initiation of a transport process that rapidly equilibrates each vesicle within the time of a single opening.[15,16]

Transport Experiment: Planar Bilayers. The ion translocation process can be directly observed using bilayer clamp techniques.[17] This type of experiment monitors the time dependence of the current carried across a planar bilayer formed in a small hole in a hydrophobic support barrier. In the presence of an active channel-type transporter, step changes in conductance indicate the "on" and "off" states of the transporter. This technique provides unambiguous demonstration of a channel mechanism and can provide molecular details of the ion translocation process.[17]

Planar bilayers were formed across an aperture in a polystyrene barrier between two aqueous salt solutions (alkali metal chlorides, typically 1 M) by painting the opening with a solution of lipid in decane. Note that the exact amount of lipid used is not known with precision, but the amounts of transporters added subsequently are unlikely to exceed 1−2 mol % of the lipid and in most cases are very much less than this amount. As the decane solution migrates up the polystyrene surface, a bilayer forms across the aperture. An electrical potential was imposed across the bilayer via two Ag/AgCl electrodes inserted into the electrolyte, and the current carried between the electrodes was monitored using a

(16) Hervé, M.; Cybulska, B.; Gary-Bobo C. M. *Eur. Biophys. J.* **1985**, *12*, 121.
(17) *Single-Channel Recording*; Sakmann, B., Neher, E., Eds.; Plenum Press: New York, 1983.
(18) Eisenman, G.; Horn, R. *J. Membr. Biol.* **1983**, *76*. 197.

Chart 1

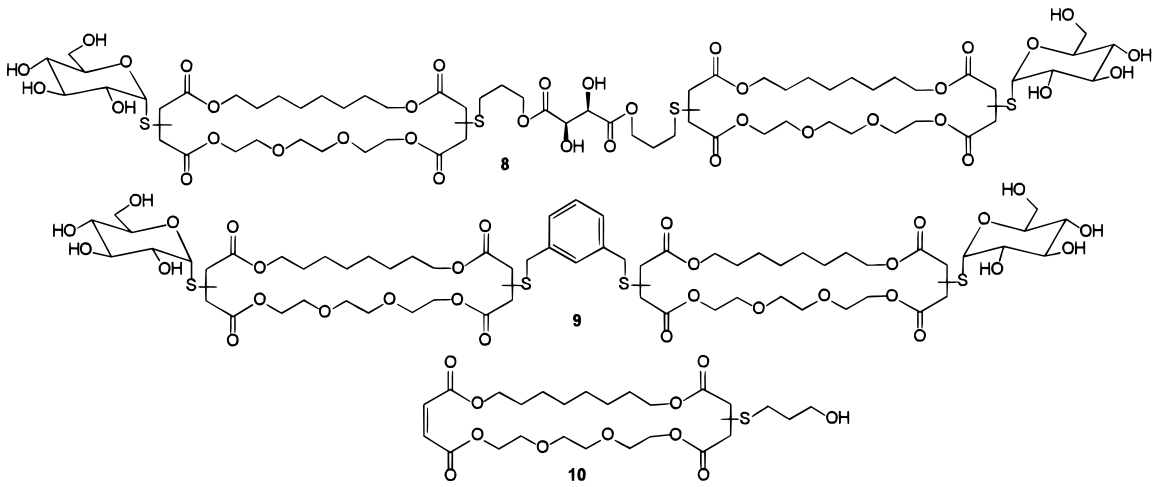

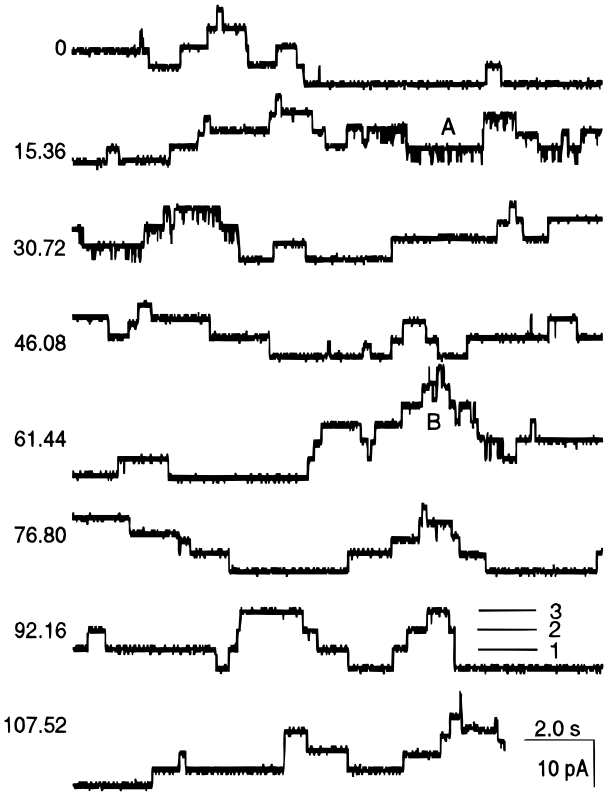

Figure 3. Example of transmembrane currents produced by **5** (3 nmol) in a diphytanoylphosphatidylcholine bilayer separating 1 M CsCl symmetrical electrolytes at 100 mV applied potential. This 2 min record occurred 15 min after addition of **5** to the cis (ground) compartment. Markers A and B and the level indicators 1−3 are discussed in the text.

bilayer clamp instrument. The bilayer is an effective insulator (GΩ) with very low conductance in the absence of added transporter (≪10 pS).

Figure 3 shows a 2 min portion of an experiment in which 40 nmol of **5** was added to a system held at a transmembrane potential of 100 mV (CsCl electrolyte, diphytanoylphosphatidiylcholine (diPhyPC)). This section of the experiment is about 15 min after the addition and is representative of a behavior sustained over periods of up to 1 h. Most significant are the step conductance changes consistent with the switching "on" and "off" of a channel-type transporter. Occasional single-channel events (square-topped peaks) occur, but the more frequently observed behavior is a series of steps of apparently the same height. Many of the openings have durations of a second or more, but some much shorter "flickering" events are evident near the point marked A in Figure 3. The total number of levels in the record is not immediately clear: near B at least six discrete levels can be seen, and more commonly three levels can be recognized as indicated by the marker in the record.

A number of features are evident in this record that apply generally to compounds **4**−**7**, NaCl, KCl, or CsCl electrolytes, and diPhyPC or PC:PA:Chol (8:1:1) as lipids. In every case, addition of methanolic solutions of the transporter to the aqueous phase results in the formation of multiple channels in 15 min or less. Controls establish that the "channels" are not due to disruption of the bilayers with methanol. There is no detectable effect of up to 4% methanol (vol/vol), whereas a typical experiment involves less than 2% methanol. In the very early stages of each experiment discrete single-channel openings are observed, but these are soon lost within the multiple openings. The multiple step behavior illustrated in Figure 3 usually persists until the bilayer ruptures (up to 2 h). In a few cases the bilayer capacitance decreases during the course of an experiment, accompanied by a loss of channel openings. Assuming a constant membrane area, decreased capacitance indicates an increase in membrane thickness. Loss of activity would correspond to the point where the bilayer exceeded the maximum span of the transporter.

What are the multiple levels of Figure 3? Are they multiple conductance states of different sized aggregates, such as are observed for alamethicin?[3b] Or are they multiple of a single species as can be observed for "high" concentrations of gramicidin?[19] Figure 4 explores these possibilities by comparing a record for **5** (3 nmol; Figure 4B) with the multiple channels from gramicidin (25 fmol; Figure 4A) and the burst openings of alamethicin single channels (0.8 nmol; Figure 4C). Both the regular level spacing and the long duration of the openings observed for **5** are similar to the openings observed for gramicidin. More importantly, the increasing level spacing, interpreted as involving successive monomer addition to alamethicin aggregates,[3] apparently does not apply to compound **5**.

The regular progression of conductance states in Figure

(19) *Ionic Channels of Excitable Membranes*; Hille, B., Ed.; Sinauer Assoc.: Sunderland, MA, 1984.

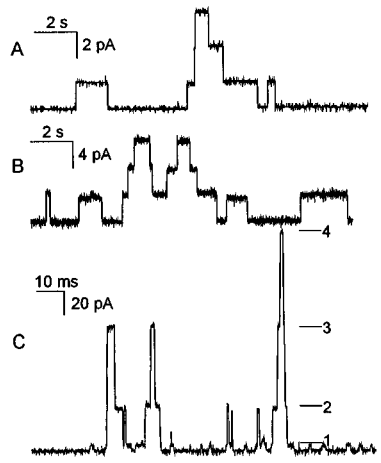

Figure 4. Comparison of transmembrane currents induced by gramicidin (A), compound **5** (B), and alamethicin (C). A: 25 fmol gramicidin, PC:PA,Chol bilayer, 1 M KCl, +120 mV. B: conditions as for Figure 3. C: 0.8 nmol alamethicin, DiPhyPC bilayer, 1 M KCl, +60 mV, levels 1−4 added as a visual aid.

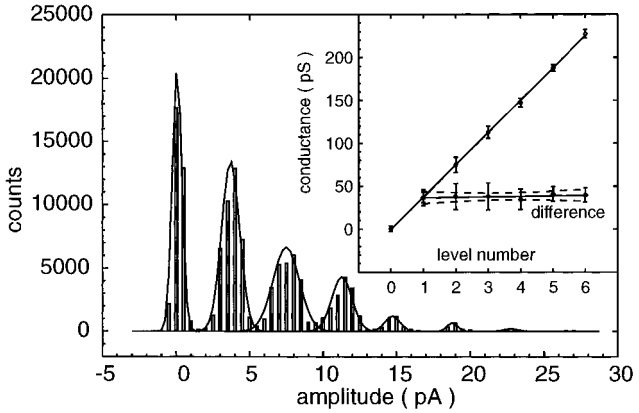

Figure 5. Amplitude histogram for the experiment of Figure 3. Curves are Gaussian fits to the histogram data. The inset shows conductance as a function of level number and conductance difference as a function of level number for this experiment as discussed in the text.

3 is more clearly indicated in the current amplitude histogram shown in Figure 5. The solid curves are calculated Gaussian fits to the clusters of peaks in the histogram. The maxima in the Gaussian fits give the current carried at each of the six levels observed, and the width yields an uncertainty. The inset to Figure 5 plots the current as a function of level to give an excellent straight line (slope = 29.3 ± 0.9 pS). That this is indeed a regular progression of equal steps is shown as a plot of the difference between steps, which is also linear (slope = −0.67 ± 0.83 pS, intercept 34.6 ± 5.1 pS).

Table 2 summarizes the specific conductances and concentration ranges required to induce multiple channels as illustrated in Figure 3, for the two different lipids (PC:PA:Chol and DiPhyPC), and with different electrolytes. The specific conductances reveal a modest cation selectivity. This is directly illustrated in Figure 6, which shows a current−voltage diagram for **5** with three electrolytes. Each point was determined from the mean step-height for multiple channel openings in the current−time record by the procedure illustrated in Figure 5. The slopes of these lines are the specific conductances reported.

The principal finding of Table 2 is that the structures of the compounds play a minor role in determining activity. There are significant differences between this suite of compounds and other channel-forming compounds under the same conditions: gramicidin requires about 50 000 times less material to form single and multiple channels (Figure 4A), and alamethicin requires about 10 times less material to form conductance bursts with resolved levels (Figure 4C).[3] Conversely, compound **8** requires about five time more material than **5** to form multiple channels similar to Figure 3 in PC:PA:Chol bilayers, compound **9** gives infrequent conductance events at 10 times the concentration in the same lipid, and compound **10** forms only erratic bursts at still higher concentrations. Differences between **4**−**7** and **8** might simply be due to different partitioning to the bilayer since the conductance records are similar in appearance. Compounds **9** and **10** induce distinctly different conductance changes, which are indicative of membrane defects and breakdown. The qualitative conclusion is that compounds **4**−**7** are closely similar, in the same way that the side-chain variants of gramicidin or alamethicin give closely similar conductance behaviors within a well-defined class.

The ionic selectivity of compounds **4**−**7** can be expressed as ratios of the conductances.[18] Alternatively, ionic selectivities can be determined from the reversal potential, V_{rev}, the potential at which there is no net ionic current in the presence of a transmembrane concentration gradient. The experiment involves creation of the bilayer between two different electrolyte solutions, for example, Cs^+ and Na^+ chlorides. The Goldman−Hodgkin−Katz equation[17−19] (eq 1) relates the reversal potential to the ion concentrations on the two sides of the membrane (subscript *cis* and *trans*):

$$V_{rev} = \frac{RT}{F} \ln\left(\frac{P_{Na}[Na^+]_{trans} + P_{Cs}[Cs^+]_{trans} + P_{Cl}[Cl^-]_{cis}}{P_{Na}[Na^+]_{cis} + P_{Cs}[Cs^+]_{cis} + P_{Cl}[Cl^-]_{trans}}\right) \quad (1)$$

where P_{Na}, P_{Cs}, and P_{Cl} are the relative permeabilities of Na^+, Cs^+ and Cl^-. For the CsCl:NaCl experiment, $[Cs^+]_{trans} = [Na^+]_{cis} = 0$ and $[CsCl]_{cis} = [NaCl]_{trans}$, so the permeability ratio of the cations is given by eq 2:

$$\frac{P_{Na}}{P_{Cs}} = \exp\left(\frac{V_{rev}F}{RT}\right) \quad (2)$$

Alternatively, the same electrolyte at two different concentrations can be used to give anion:cation permeability ratios by direct substitution of concentrations in eq 1. Table 3 gives permeability ratios calculated from V_{rev} for **4**−**7**, in comparison with conductance ratios calculated from the data of Table 2.

Several structurally related trends are apparent. Firstly, the marked K^+:Cl^- selectivity of **5** must be related to its net charge (2−) relative to the monoanionic (**4**, **7**) and zwitterionic (**6**) members of the series. Secondly, compound **4** shows very significant discrimination against Na^+ relative to the other compounds. This must stem from the single head-group on **4** relative to the bola-amphiphiles in the rest of the group. Note also that the permeability ratios, determined for two cations in competition, are greater than the conductance ratios determined for individual electrolytes. This is a significant excursion from systems such as gramicidin where the

Table 2. Amounts Required and Specific Conductance of Multiple Channels in Planar Bilayers[a]

compd	amt required[b] (nmol)	specific conductance[b] 1 M KCl (pS)	amt required[c] (nmol)	specific conductance[c] 1 M CsCl (pS)	specific conductance[c] 1 M KCl (pS)	specific conductance[c] 1 M NaCl (pS)
4	5−10	10.7 ± 0.4	20−30	32.9 ± 0.3	15.5 ± 0.4	7.7 ± 0.3
5	3−5	14.6 ± 0.3	30−40	29.3 ± 0.9	15.0 ± 0.5	9.9 ± 0.3
6	0.5−1	12.5 ± 0.5	20	32.5 ± 0.5	15.8 ± 1.1	9.0 ± 0.2
7	10	13.0 ± 0.3	30−40	33.1 ± 0.6	16.3 ± 0.4	9.4 ± 0.4

[a] Bilayer was formed from a decane solution of the lipid indicated at 298 K. The transporter was added as a solution in methanol. Conductance events occur within in 15 min at the lowest concentration given. [b] Bilayer formed from phosphatidylcholine:phosphatidic acid:cholesterol (8:1:1). [c] Bilayer formed from diphytanoylphosphatidylcholine.

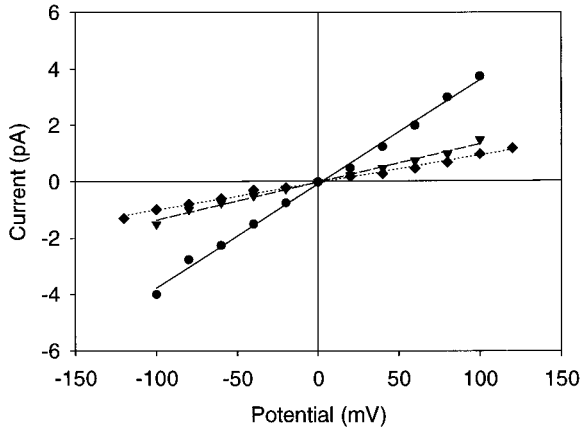

Figure 6. Current−voltage diagram for **5** in diphytanoylphosphatidylcholine bilayers for CsCl (filled circle), KCl (filled triangle), and NaCl (diamond) electrolytes.

converse is normally observed.[3,19] This implies that the conducting pores in this series are flexible and swell or shrink to accommodate a particular cation as it passes. When all ions are of the same type, no reorganization is required. Between competing cations, reorganizational barriers would tend to favor ions of a similar type following one another. If this is the case, the selectivities require that expansion would be less unfavorable than contraction. The postulate of cation dependent channel structure is consistent with a few observations of several types of channels, with different conductivities, in the opening seconds of experiments with **4** in membranes between NaCl and CsCl. Unfortunately, the large numbers of openings that follow mask the single-channel differences.

Mechanism. Our initial assumption is that the mode-of-action for cation transport by these bola-amphiphiles is the same for both planar and curved (vesicle) bilayer membranes. This apparently poses a problem since the ion selectivity sequences determined in the two systems are different. We relate this difference to the very different nature of the kinetic processes being observed in the two experiments. Single-channel experiments examine the ion permeability directly and, in a multiple channel case such as this, provide relatively little information about the initiation of channel openings. Conversely, vesicle experiments assume that channel activity is high[11,15,16] so the kinetics report only the initiation events. The high activity assumption is clearly valid in this system. A single 15 pS channel under a 60 mV transmembrane potential carries 5×10^6 ions/s. A 350 nm diameter vesicle with our buffer system maintains a 1 pH unit gradient (equivalent to 60 mV of transmembrane potential) based on 5×10^5 protons. Thus, a single 100 ms opening of a 15 pS channel would be sufficient to equilibrate a 350 nm vesicle. The openings in Figure 3 are 10−40 times longer than this lower boundary. The ion selectivity differences between planar and vesicle bilayers must therefore relate to differences between the cation dependence of initiation of channels and the actual selectivity of the channel for ion translocation.

The apparent kinetic order results in vesicles imply that the active structures are aggregates of bola-amphiphile monomers. The uniformity of the step-conductance changes observed in planar bilayer systems implys that the active structures are remarkably uniform. The simplest model consistent with both results would therefore involve the formation of an active dimer. More complex models might involve active trimers, tetramers, and higher oligomers. However, a model of oligomers in equilibrium with monomers, such as is postulated for alamethicin,[3] is not supported by the data. In such a model, each additional monomer that adds enlarges the pore; thus, each additional monomer increases the conductance. The increase cannot be linear: trimer to tetramer will involve a different conductance increase from pentamer to hexamer. A plot of the difference in conductance between levels as a function of level number, similar to the inset of Figure 5, would be expected to level off at high level number.[3] There is no evidence for that behavior in this system, and we interpret Figure 5 as evidence directly against such a model. The alternative model of multiple copies of a discrete species is more consistent with the data. We observe no subconductance states[3] so the active state must form in a single step from inactive states. The active species is presumably a small aggregate or cluster (dimer, trimer) that can support a transmembrane water channel adjacent to or within the cluster. The cluster is envisaged as a less structured version of the four- and five-bundle peptide helices proposed in other systems.[8] This suite of compounds lacks suitable spectroscopic probes to determine any feature of the proposed aggregate.

Considered step-by-step, the process must involve diffusion of the bola-amphiphile to the membrane, insertion into the bilayer, and aggregation to form the active structure. Figure 7 illustrates some possible intermediate stages for a symmetrical compound such as **5**. Other orientations become possible when the two head-groups are different, but we ignore those refinements here. State A is simply the result of the diffusion step: no specific interaction of bola-amphiphile and membrane is implied or precluded. The insertion step to the U-shaped state B is a logical possibility, followed by a penetration of one of the head-groups to generate the transmembrane state C. An alternative would be a "threading" insertion to generate the trans-membrane state C directly from A. A second head-group penetration would generate another U-shaped state on the other side of the bilayer. Provided the insertion proceeds one molecule at a time, the aggregate model requires that states A to D must all be inactive for cation translocation. We have no direct

Table 3. Ion Selectivity of Transporters[a]

compd	Cs:Na conductance ratio	Cs:Na permeability ratio	K:Na conductance ratio	K:Na permeability ratio	K:Cl permeability ratio
4	4.3 ± 0.3	32 ± 1	2.0 ± 0.2	24 ± 1	9 ± 5
5	3.1 ± 0.3	8.3 ± 0.4	1.5 ± 0.2	*b*	25 ± 4
6	3.6 ± 0.3	6.5 ± 0.5	1.7 ± 0.3	3.9 ± 0.3	9.5 ± 0.5
7	3.5 ± 0.4	5.5 ± 1.0	1.7 ± 0.4	1.1 ± 0.3	8 ± 5

[a] Conductance ratios determined from the data of Table 2; permeability ratios determined from reversal potentials as described in the text. Diphytanoylphosphtidylcholine bilayers, 300 K. [b] Not determined.

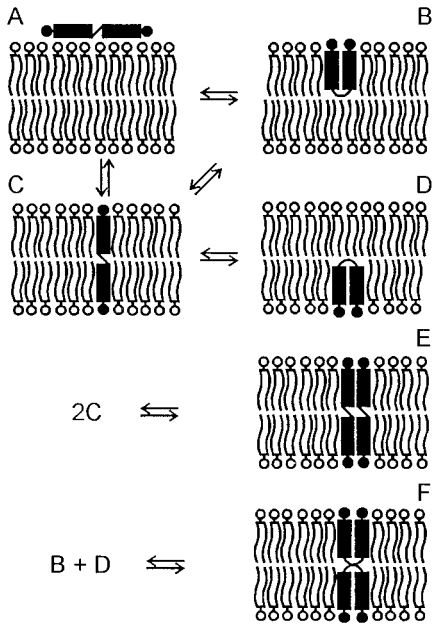

Figure 7. Schematic of steps leading to pore formation.

evidence on the rates of these steps, but assume them to be slower that the channel initiation steps which follow. In general, transmembrane motions of lipids are slower than lateral diffusion rates by several orders of magnitude.[21]

From these inactive states, the side-to-side aggregation to generate the dimer (state E) would result in the initiation of cation transport. An alternative would involve dimerization of the two U-shaped states to generate state F. A further alternative (not illustrated) would involve the side-to-side dimerization of B or D. We view this last possibility as unlikely since U-shaped insertion of bola-amphiphiles is implicated in the membrane disrupting systems reported by Regen.[14] Our own investigation of bola-amphiphilic bis-crown ethers supports the role of state B as a precursor for membrane disruption.[20] The processes illustrated in Figure 7 are akin to the mechanism presented for Kobuke's aggregate pores.[12] The additional features of this system are the formation of discrete conducting aggregates leading to ion-selectivity.

The questions posed in the introduction focused on the potential for aggregation of bola-amphiphiles as a means to create active and selective channels with modest synthetic effort. That potential has been partially realized in this system, and the insights gained point to further structural variations to test the proposed mechanism directly. The proposed mechanism also indicates ways to introduce control elements for switching. For example, a U-shaped to linear switch, such as photoisomerization, would control the B to C equilibrium. Our further explorations in this area will be reported in due course.

(20) Fyles, T. M.; Zeng, B. *J. Chem. Soc., Chem. Commun.*, in press.
(21) Moss, R. A. *Pure Appl. Chem.* **1994**, *66*, 851 and references therein.

Experimental Section

Proton NMR spectra were recorded at 250, 300, or 360 MHz in $CDCl_3$ or CD_2Cl_2. Carbon NMR spectra were recorded at 62.89, 75.48, or 90.57 MHz in $CDCl_3$ or CD_2Cl_2. Negative-ion LSIMS (−FAB) mass spectra were recorded in *meta*-nitrobenzyl alcohol (mNBA) as matrix. Elemental analyses were performed by Canadian Microanalytical Services, New Westminster, B.C. In addition to the data reported, all samples ran as single sharp peaks on an analytical gel permeation column (mixed-bed polydivinylbenzene, 10 mm i.d. × 25 cm) with $CHCl_3$ as eluent. These gel permeation conditions can resolve products differing by >50 g/mol in the molecular weight range of 500 to 2000 g/mol. Compounds **1** and **2** have been previously reported.[6] The lipids used were obtained from Avanti Polar Lipids, were stored under Ar at 253 K, and were used within 2 months of receipt: egg phosphatidyl choline (PC), egg phosphatidic acid (PA), diphytanoylphospatidylcholine (DiPhyPC).

Bis[3- or 4-, 17- or 18-(2-carboxy-1-thiaethyl)]-1,6,9,12,15,20-hexaoxa-2,5,16,19-tetraoxocyclooctacosane (3). Compound **1** (1.50 g, 3.29 mmol) and 2-mercaptoacetic acid (1.84 g, 20 mmol, 6 equiv) were added to dried tetrahydrofuran (250 mL). 2,2,6,6-Tetramethylpiperidine (2.2 mL) was added, and the mixture was stirred at 60 °C under nitrogen for 6 h. The tetrahydrofuran was removed under reduced pressure. The pale yellow mixture was dissolved in 2-propanol:chloroform (3:4) and added to a cation-exchange resin (Dowex 50 × 8, 100, 2 × 22 cm) that had been activated with 2 M sulfuric acid and washed with water, 2-propanol, and a 3:4 mixture of 2-propanol:chloroform. The acidic fractions were combined, concentrated to ∼2 mL, and purified on a gel permeation column (LH-20, 3 × 20 cm) using 2-propanol:chloroform (3:4) as eluent. Product **3** was obtained in the early fractions as a colorless oil. The product of mono-addition was obtained in the middle fractions as a pale yellow oil. The last fractions contained unreacted **1**. The product-containing fractions were evaporated to give **3** as a colorless oil (1.14 g, 1.78 mmol, 54%): ^{1}H NMR 300 MHz (δ, $CDCl_3$) 9.37 (br s, 2H), 4.21−4.00 (m, 8H), 3.82−3.77 (m, 2H), 3.63−3.58 (m, 8H), 3.52−3.27 (m, 4H), 2.95−2.61 (m, 4H), 1.55−1.53 (m, 4H), 1.22 (m, 8H); ^{13}C NMR 75.48 MHz (δ, $CDCl_3$) 173.6−170.0 (seven peaks), 70.1, 68.7, 65.6, 65.5, 65.4, 64.9, 64.3, 63.7, 41.7, 41.5, 35.9, 35.7, 33.1, 32.8, 28.4, 28.1, 25.4, 25.2; MS (−FAB, mNBA) 639.1 $(M - H)^-$ 100; exact mass calcd for $(M - H)^-$, $C_{26}H_{39}O_{14}S_2$, *m/e* 639.1781, found *m/e* 639.1832.

3- or 4-[8′-[17″- or 18″-(2‴-Carboxy-1‴-thiaethyl)-1″,6″,9″,12″,15″,20″-hexaoxa-2″,5″,16″,19″-tetraoxocyclooctacos-3″- or 4″-yl]-6′-oxo-5′,1′,8′-oxadithiaoctyl]-1,6,9,12,15,20-hexaoxa-2,5,16,19-tetraoxocyclooctacosa-17-ene (4). Tetramethylammonium pentahydrate (0.29 g, 1.60 mmol) was dissolved in DMSO (5 mL) at 40 °C under nitrogen and mixed with **3** (1.02 g, 1.59 mmol, 1 equiv) in DMSO (7 mL). Compound **2** (1.00 g, 1.60 mmol, 1 equiv) in DMSO (8 mL) was added dropwise, and the mixture was held at 40 °C under nitrogen for 25 h. The solvent was removed under reduced pressure. The brown mixture was dissolved in chloroform (300 mL), washed with 1 M hydrochloric acid (5 × 150 mL), and

dried over magnesium sulfate, and the solvent was removed. The light brown oil was chromatographed on a gel permeation column (LH-20, 3 × 20 cm), and the product was eluted with 2-propanol:chloroform (3:4). A diene product of double reaction was obtained in early fractions. The desired **4** was obtained in the middle fractions, and unreacted **3** was obtained in the last fractions. The product-containing fractions were evaporated to give **4** as a yellow oil (0.22 g, 0.19 mmol, 12%): ^{1}H NMR 300 MHz (δ, $CDCl_3$) 7.88 (br s, 1H), 6.76, 6.17 (s, 2H), 4.26−3.94 (m, 18H), 3.84−3.53 (m, 19H), 3.50−3.23 (m, 4H), 2.95−2.55 (m, 8H), 1.95−1.86 (m, 2H), 1.55 (m 8H), 1.24 (m, 16H); ^{13}C NMR 75.48 MHz (δ, $CDCl_3$) 172.1−169.3 (14 peaks), 165.2−164.6 (5 peaks), 133.8, 132.9, 130.1, 129.9, 129.1, 128.9, 70.5−70.0 (5 peaks), 68.8, 68.7, 65.6, 65.3, 65.2, 65.1, 64.7, 64.4, 64.2−63.6 (six peaks), 41.9, 41.5, 41.4, 41.2, 36.3, 36.1, 35.9, 35.7, 33.5, 33.0, 32.9, 29.4, 28.6, 28.5, 28.1, 27.8, 27.7, 27.5, 25.5, 25.3, 25.2; MS (−FAB, mNBA) 1078.4 $(M - head)^-$ 1.4, 1169.4 $(M - H)^-$ 20.7, 1212.5 $(M + 43 - H)^-$ 2.1; exact mass calcd for $(M - H)^-$, $C_{51}H_{77}O_{24}S_3$, *m/e* 1169.3967, found *m/e* 1169.4041. Anal. Calcd for $C_{51}H_{78}O_{24}S_3$: C, 52.30; H, 6.71; S, 8.21. Found: C, 52.17; H, 6.56; S, 8.28.

3- or 4-[8′-[17″- or 18″-(2‴-Carboxy-1‴-thiaethyl)-1″,6″,9″,12″,15″,20″-hexaoxa-2″,5″,16″,19″-tetraoxocyclooctacos-3″- or 4″-yl]-6′-oxo-5′,1′,8′-oxadithiaoctyl]-17- or 18-(2-carboxy-1-thiaethyl)-1,6,9,12,15,20-hexaoxa-2,5,16,19-tetraoxocyclooctacosane (5). Compound **4** (0.090 g, 0.077 mmol) and 2-mercaptoacetic acid (0.025 g, 0.27 mmol, 3.5 equiv) were dissolved in dried tetrahydrofuran (5 mL). 2,2,6,6-Tetramethylpiperidine (0.7 mL) was added, and the solution was stirred for 5 h at 60 °C under nitrogen. The tetrahydrofuran was removed under reduced pressure, the light yellow mixture was dissolved in dichloromethane (150 mL), washed with 1 M hydrochloric acid (5 × 70 mL), and dried over magnesium sulfate, and the solvent was removed to give a light yellow oil. The crude product was chromatographed on a gel permeation column (LH-20, 3 × 20 cm) eluted with a solvent of 2-propanol:chloroform (3:4). The middle fractions containing the expected product were evaporated to give **5** as a light yellow oil (0.040 g, 0.032 mmol, 42%): ^{1}H NMR 360 MHz (δ, $CDCl_3$) 5.12 (br s, 2H), 4.24−4.09 (m, 18H), 3.84−3.34 (m, 26H), 3.00−2.65 (m, 10H), 1.94 (m, 2H), 1.61 (m, 8H), 1.30, 1.24. 1.22 (m, 16H); ^{13}C NMR 90.57 MHz (δ, $CDCl_3$) 172.1−169.6 (10 peaks), 70.5, 70.3, 70.1, 69.3, 69.1, 68.9, 65.6, 65.4, 65.0, 64.7, 64.2, 64.1, 63.9, 63.7, 42.4, 41.7, 41.6, 36.4, 35.9, 33.9, 33.6, 33.5, 33.2, 32.9, 31.9, 31.7, 29.6, 29.3, 28.6, 28.3, 28.1, 27.9, 25.5, 25.3, 22.6, 21.7, 14.1; MS (−FAB, mNBA) 1261.4 $(M - H)^-$ 100, 1303.4 $(M + 43 - H)^-$ 23.5; exact mass calcd for $(M - H)^-$, $C_{53}H_{81}O_{26}S_4$, *m/e* 1261.3899, found *m/e* 1261.3912.

3- or 4-[8′-[17″- or 18″-(2‴-Carboxy-1‴-thiaethyl)-1″,6″,9″,12″,15″,20″-hexaoxa-2″,5″,16″,19″-tetraoxocyclooctacos-3′- or 4′-yl]-6′-oxo-5′,1′,8′-oxadithiaoctyl]-17- or 18-(*N*,*N*-dimethyl-3,1-azathiapropyl)-1,6,9,12,15,20-hexaoxa-2,5,16,19-tetraoxocyclooctacosane (6). Compound **4** (0.19 g, 0.16 mmol) and 2-(dimethylamino)ethanethiol hydrochloride (0.092 g, 0.65 mmol, 4 equiv) were mixed in 2-propanol (15 mL). 2,2,6,6-Tetramethylpiperidine (1 mL) was added, and the mixture was heated at reflux for 2 h under nitrogen. The solvents were evaporated, the crude product was dissolved in chloroform (200 mL), washed with 1 M hydrochloric acid (5 × 100 mL), and dried with magnesium sulfate, and the solvent was removed to give a pale yellow oil. Gel permeation (LH-20, 3 × 20 cm) of the product eluted with 2-propanol:chloroform (3:4) gave the purified material near the void volume. The combined product-containing fractions were evaporated to give **6** as a pale yellow oil (0.14 g, 0.11 mmol, 68%): ^{1}H NMR 250 MHz (δ, $CDCl_3$) 4.23−4.07 (m, 18H), 3.85−3.25 (m, 30H), 3.02−2.63 (m, 14H), 1.96−1.93 (m, 2H), 1.61 (m, 8H), 1.30, 1.26, 1.22 (m, 16H); ^{13}C NMR 62.89 MHz (δ, $CDCl_3$) 171.2−169.4 (five peaks), 70.5, 68.9, 65.8, 65.5, 65.3, 65.0, 64.9, 64.6, 64.4, 64.1, 63.9, 56.9, 43.0, 41.9, 41.8, 36.6, 36.4, 36.2, 36.1, 34.1, 33.6, 33.2, 28.7, 28.3, 28.1, 28.0, 27.8, 25.6, 25.5, 25.4, 21.7; MS (−FAB, mNBA) 1274.6 $(M - H)^-$; exact mass calcd for $(M - H)^-$, $C_{55}H_{88}O_{24}NS_4$, *m/e* 1274.4579, found *m/e* 1274.4677.

3- or 4-[8′-[17″- or 18″-(2‴-Carboxy-1‴-thiaethyl)-1″,6″,9″,12″,15″,20″-hexaoxa-2″,5″,16″,19″-tetraoxocyclooctacos-3′- or 4′-yl]-6′-oxo-5′,1′,8′-oxadithiaoctyl]-17- or 18-[(β-D-glucosyl)thio]-1,6,9,12,15,20-hexaoxa-2,5,16,19-tetraoxocyclooctacosane (7). Compound **4** (100 mg, 0.086 mmol) was dissolved in dry THF:2-propanol (50:50, 10 mL). 1-Thio-β-D-glucose sodium salt dihydrate (43.9 mg, 0.17 mmol, 2 equiv) was added, followed by methane sulfonic acid (17.6 mg, 0.18 mmol, 2.1 equiv) in 2-propanol (1 mL). The mixture was stirred at 50 °C under nitrogen for 1.5 h, 2,2,6,6-tetramethylpiperidine (0.7 mL) was added, and the reaction was held a further 16 h at 50 °C. After the solvent was removed, the crude product was dissolved in dichloromethane (100 mL), washed with 1 M hydrochloric acid (3 × 50 mL), and dried with sodium sulfate. Dichloromethane was removed, and the yellow oil was chromatographed in three portions on a gel permeation column (LH-20, 3 × 20 cm) eluted with 2-propanol:chloroform (3:4). In each portion, the expected product was collected among the middle fractions. The combined products were evaporated to give **7** as a pale yellow oil (0.045 g, 0.033 mmol, 38%): ^{1}H NMR 360 MHz (δ, CD_2Cl_2) ∼5 (v br, 4H), 4.24−4.10 (m, 18H), 3.94−3.60 (m, 23H), 3.57−3.37 (m, 8H), 3.01−2.69 (m, 10H), 1.94 (m 2H), 1.62 (m, 8H), 1.32 , 1.25, 1.23 (m, 16H); ^{13}C NMR 90.57 MHz (δ, CD_2Cl_2) 172.4−169.9 (13 peaks), 85.2, 84.3, 80.1, 78.1, 72.8, 70.8, 70.7, 70.6, 69.9, 69.3, 69.2, 66.5, 66.2, 66.0, 65.9, 65.7, 65.5, 65.3, 65.1, 64.9, 64.8, 64.5, 64.4, 64.2, 62.1, 42.6, 42.2, 42.0, 41.8, 40.7, 37.7, 36.9, 36.8, 36.7, 36.5, 36.4, 36.3, 33.9, 33.6, 33.5, 33.4, 30.0, 29.2, 29.1, 28.7, 28.5, 28.3, 28.1, 25.9, 25.8, 25.7, 21.8; MS (−FAB, mNBA) 1365.4 $(M - H)^-$ 66.5; exact mass calcd for $(M - H)^-$, $C_{57}H_{89}O_{29}S_4$, *m/e* 1365.4372, found *m/e* 1365.4400.

Vesicle Experiments. The solutions, preparation methods, characterization methods, data acquisition, and data analysis methods are described in detail in refs 11 and 15. The transporters (**4**−**7**) were dissolved in methanol to a concentration of 5 mM. This permits the active concentration range to be achieved by addition of <25 μL to the 5 mL of solution contained in the pH-stat cell (0.5 vol/vol % methanol). Typically, the transporter was added at 0.3 mol % of the lipid.

Planar Bilayer Experiments. Single channel currents were measured with a BC-525A bilayer clamp (Warner Instrument Corp.) using Ag/AgCl electrodes inserted into the electrolyte held in a bilayer chamber (Warner Instrument Corp. BCH-22; polystyrene, 0.25 mm hole size, 2.5 mL volume). Bilayer formation was monitored on an oscilloscope with a 100 Hz square-wave using the capacitance test function of the bilayer clamp. The signal was analog filtered using an eight-pole lowpass Bessel filter (Model 902, Frequency Devices), digitized using a Digidata 1200 A/D board, and acquired using the pClamp6 suite of programs (Axon Instruments).

Lipid dispersions (17 mg/mL) were formed by evaporating stock solutions of lipid in $CHCl_3$ and redissolving the lipid in decane using sonication if required. The aperture of the dry bilayer cell was prepainted with the lipid dispersion and dried under a stream of nitrogen. Electrolyte was added to the cell, and the circuit was completed. The bias of the bilayer clamp was adjusted to compensate for junction potentials, and then a drop of lipid dispersion was spread across the aperture using a fine paint brush. Any excess was removed by brushing with a clean brush. The capacitance was monitored until stable (0.3−0.45 μF/cm^2), followed by a period of base-line monitoring. Bilayers with a conductance greater than 10 pS were not used for transport studies. Methanolic solutions of transporters ((1−5) × 10^{-4} M) were added by microliter syringe to the cis compartment of the chamber. Potentials were applied relative to the cis compartment (as ground).

Initially, the current−time records were analyzed manually to determine the current step-height at each applied potential. Linear least-squares fit to the data gave the specific conductance. In a later phase, the current−time record was treated using the Fetchan program (Axon) to give Gaussian fits to the amplitude histograms. The two methods were found to be equivalent within the errors indicated in Tables 2 and 3.

Reversal potentials were measured on bilayers formed between the two different electrolytes by setting the applied potential at a high value (100 mV) until clear channel activity was established and then manually adjusting the applied potential to a point where no channels were observed. The reversal potential was approached manually from both directions. Following this manual estimation of the potential, a triangle-wave voltage ramp crossing the region of interest was applied, and a current−voltage diagram was constructed as an average of 20 cycles. The voltage intercept was taken as the reversal potential. The manual and averaged values typically agreed within ± 2 mV. Observed reversal potentials (electrolyte$_{cis}$:electrolyte$_{trans}$, V_{rev} (mV), all solutions 1 M unless indicated otherwise): **4**, NaCl:CsCl, 89 ± 0.7; NaCl:KCl, 81.2 ± 0.2; 0.1 M KCl:0.5 M KCl, 31.1 ± 3.4; **5**, NaCl:CsCl, 54.4 ± 1.1, 0.1 M KCl:0.5 M KCl, 36.8 ± 0.6; **6**, CsCl:NaCl, −44 ± 2; KCl:NaCl, −21 ± 2; 0.1 M KCl:0.5 M KCl, 31.1 ± 0.6; **7**, NaCl:CsCl , 48 ± 2; NaCl:KCl, 35 ± 2; 0.1 M KCl:0.5 M KCl, 29.8 ± 6.

Acknowledgment. The ongoing support of the Natural Sciences and Engineering Research Council of Canada is gratefully acknowledged.

Supporting Information Available: ^{1}H and ^{13}C NMR spectra of compounds **3**−**7** (11 pages). This material is contained in libraries on microfiche, immediately follows this article in the microfilm version of the journal, and can be ordered from the ACS; see any current masthead page for ordering information.

JO961267C